NUCLEAR SCIENCE AND TECHNIQUES **25**, 050502 (2014)

Density functional theory study of H, C and O chemisorption on UN(001) and (111) surfaces*

LI Ru-Song (李如松),[1,†] HE Bin (何彬),[1] XU Peng (许鹏),[1] WANG Fei (王飞),[1] and MA Wen-Yan (马文彦)[1]

[1] *Xi'an Research Institute of Hi-Tech, Xi'an 710025, China*

(Received March 28, 2014; accepted in revised form June 27, 2014; published online October 4, 2014)

We performed density functional theory calculations of H, C, and O chemisorption on the UN(001) and (111) surfaces using the generalized gradient approximation (GGA) and the Hubbard U parameter and revised Perdew-Burke-Ernzerhof (RPBE) exchange-correlation functional at non-spin polarized level with the periodic slab model. Chemisorption energies vs. distance of molecules from UN(001) and UN(111) surfaces have been optimized for four symmetrical chemisorption sites, respectively. The results show that the Hollow, N-top, and Hollow adsorption sites are the most stable sites for H, C, and O atoms with chemisorption energies of 13.06, 25.50 and 27.34 kJ/mol for UN(001) surface, respectively. From the point of adsorbent (UN(001) and UN(111) surfaces in this paper), interaction of O with the chemisorbed surface is of the maximum magnitude, then C and H, which are in agreement with electronegativities of individual atoms. For the UN(001) surface, U-N bond lengths change relatively little ($< 9\%$) as a result of H chemisorption, however C and O chemisorptions result in remarkable changes for U-N bond lengths in interlayer ($> 10\%$). Electronic structure calculations indicate that Bridge position is equivalent with Hollow position, and the most stable chemisorption position for H, C, and O atoms are all Bridge (or Hollow) position for the UN(111) surface. Calculated electronic density of states (DOSs) demonstrate electronic charge transfer between s, p orbitals in chemisorbed atoms and U $6d$, $5f$ orbitals.

Keywords: Chemisorption, Density functional theory, Relaxation, Density of states

DOI: 10.13538/j.1001-8042/nst.25.050502

I. INTRODUCTION

Uranium nitrides are considered as promising fuel for the fast nuclear Generation IV reactors. Compared to many uranium and plutonium oxide nuclear fuels, uranium nitrides have several advantages [1, 2], such as higher thermal conductivity, melting point, metal density, and smaller lattice constant. Many research groups have identified an important role of UN in anti-corrosion application since the 1960s [3–5], and investigations on uranium nitride compounds renew great attention due to enviormental pollution and increasing interest for development of new nuclear fuels. The bulk properties of actinide nitrides have been investigated in these works, especially the elastic and magnetic properties.

Contrary to a number of available experimental data, some theoretical work have paid much attention on the pure and defective UN, physical properties of various defects (such as vacancy, O impurities, grain boundary) [6–13]. Basic bulk properties have been considered in these studies for uranium nitrides with emphasis on elastic and magnetic properties [14–18]. Petit *et al*. [9] have clarified the partial localization of $5f$ electrons in UN and reproduced the experimental total magnetic moment. In Ref. [7], the all-electron relativistic spin-polarized DFT calculations were performed to evaluate the total energies, optimized geometries, and electronic and thermodynamic properties of perfect stoichiometric UN and UN_2 single crystals. However, high reactivities of uranium nitrides with hydrogen, carbon, and oxygen at ambient atmosphere can affect the fuel fabrication process and fuel performance [1]. Experimental studies also clearly showed that oxygen in contact with the surface of uranium mononitride can result in growth of the oxide compound and, in initial stages, can lead to the formation of a surface layer structurally similar to oxynitrides UO_xN_y [19].

To predict UN fuel performance under different operating conditions and understand the material properties at the microscopic scale, it is crucial to investigate the surface properties and chemisorption process based on electronic structure calculations. However, a few papers have focused on the chemisorption behaviors of molecules or atoms on the surface of uranium nitrides.

Only recently [19–23], some groups have simulated the reactivity of molecules/atoms with the surface of uranium nitrides. These reports have indicated that O_2 molecule would spontaneously dissociate after chemisorption on the UN(001) surface, then the produced O atoms exhibit a strong chemisorption behavior.

According to Tasker's analysis, the (001) surface must have the lowest surface energy for the rock-salt compounds [24]. At the same time, the (111) surface is usually the most dense plane for face-centered cubic (fcc) structure. Therefore, we consider two representative planes for the UN lattice–UN(001) and UN(111) surface. In this work, we perform electronic structure calculations within the framework of density functional theory (DFT) method to deeply understand chemisorption mechanisms of H, C, and O atoms on the UN(001) and (111) surfaces, shed light on the mechanisms of hydrogenization, oxidation, and cabonization of UN in the air at the electronic and atomic level, and analyse the chemical bonding of U $6d$, $5f$ states with H $1s$, C $2s$, $2p$, and O $2s$, $2p$ states.

* Supported by National Natural Science Foundation of China (Nos. 51401237, 51271198 and 11474358) and Self-Topics Fund of Xi'an Research Institute of High Technology (Nos. 2014QNJJ018 and YX2012cxpy06)

† Corresponding author, rusong231@126.com

II. METHODOLOGY

Uranium mononitride (UN) has NaCl-type structure (face-centered cubic) with the experimental lattice constant $a = 0.4889$ nm. In this paper, we use the generalized gradient approximation (GGA) + U (Hubbard U parameter to represent a correction to Coulomb repulsion interaction, separating f manifold into lower and upper Hubbard bands and removing f degrees of freedom from the Fermi level, $U = 4.0$ eV) within the framework of density functional theory (DFT) and revised Perdew-Burke-Ernzerhof (RPBE) exchange-correlation functional with a periodic $\sqrt{2} \times \sqrt{2}$ three-layer slab model and single-sided chemisorption mode (an atom is placed on one side of the slab model, namely 0.5 ML adsorptivity) to simulate chemisorption behaviors of H, C, and O atoms on UN(001) and (111) surfaces in all calculations. A vacuum layer of 2.0 nm is added to a unit cell of the layers. The vacuum height test will be described in Sec. III in detail. We do not yet consider fully relativistic effects instead by using the scalar-relativistic approach. However, all other relativistic kinematic effects, such as mass-velocity, Darwin, and higher order terms are retained. Wang and Hay *et al*. [25, 26] have found that one can adequately describe the electronic and geometric properties of actinide complexes without treating spin-orbit effects explicitly, since we are interested in the chemisorption energies, defined as the difference in total energies. Therefore, we expect the inclusion of other relativistic effects, such as spin-orbit coupling, spin polarization, and orbital polarization effects, will not alter the main qualitative and quantitative conclusions of our work, as discussed in other works [27].

The outer fourteen electrons ($6s^2 6p^6 5f^6 6d^1 7s^2$) of the U atom are treated as the valence electrons and the remaining seventy-eight electrons are treated as the core electrons. DFT semi-core pseudopotentials (DSPP) and a double numerical basis set with polarization functions (DNP) have been used to treat the core electrons and the valence electrons, respectively. All electron basis sets are used for H, C, N, and O atoms. A $8 \times 8 \times 2$ Monkhorst-Pack k-point mesh is applied for the Brillouin zone (BZ) integration. The convergence of a self-consistent field (SCF) is less than 1.0×10^{-5} eV/atom. A plane-wave cutoff energy is fixed at $E_{\text{cut}} = 500$ eV, which is enough for convergence of chemisorption calculations. Non-magnetic configuration is appropriate for the light actinide U element from the point of total energy, so U $5f$ electrons are in the delocalized $5f^3$ electronic configuration in the present work.

Single atom, one per unit cell, is allowed to approach the UN(001) surface along four different symmetrical positions, namely (I) on the middle of the two nearest U atoms (Bridge position), (II) the adsorption atom sees a U atom located on the layer directly below the surface hollow site (Hollow position), (III) directly on top of a U atom (U-top position), and (IV) directly on top of a N atom (N-top position), as shown in Fig. 1, whereas only the former three symmetrical chemisorption positions exist for the UN(111) surface (not shown here). Chemisorption energy E_{C} is optimized with respect to the height R of the chemisorbed atom above the surface, and is

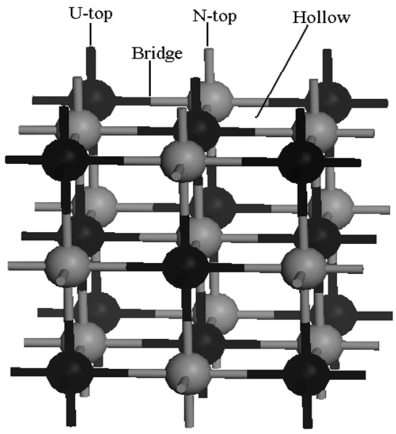

Fig. 1. UN(001) surface has four symmetrical chemisorption positions, namely Bridge, Hollow, U-top and N-top, whereas only the former three symmetrical chemisorption positions exist for UN(111) surface.

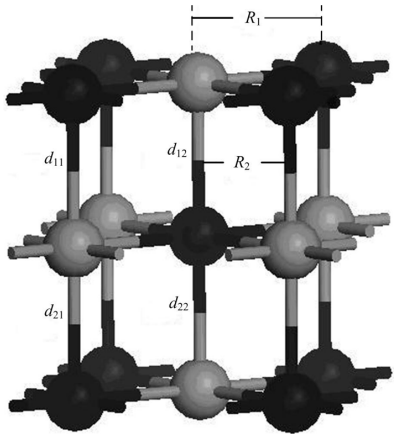

Fig. 2. A configuration model for relaxation calculation. R_i ($i = 1$, 2) and d_{ij} ($i = 1$, 2, $j = 1$, 2) represent U-N bond length in the intralayer and interlayer, respectively.

given by [28]

$$E_{\text{C}}(R) = E(M) + E(\text{X}) - E(M{+}X), \tag{1}$$

where $E(M)$ is total energy of a bare UN(001) or UN(111) slab, $E(X)$ is the total energy of the isolated atom in reference crystal structure, and $E(M{+}X)$ is the total energy of the entire chemisorption system.

The relative change for bond length is utilized to describe the change for U-N bond length as a result of atom chemisorption

$$\Delta = (R_i - R_0)/R_0, \tag{2}$$

where R_i is the bond length for the central N atom on the UN(001) surface and the i^{th} U atom, R_0 is the original U-N bond length, and Δ denotes the relative change for R_i. The serial numbers i are shown in Fig. 2.

III. CONFIGURATIONS FOR UN(001) AND (111) SURFACES

To test the validity of the computational parameters, we first cleave the UN(001) surface, then check the convergence of total energy of the UN(001) surface with different vacuum thicknesses. We consider a vacuum thickness test to be convergent as long as change for total energy ΔE is less than 10 meV. Test results indicate that the total energy of a system is convergent when vacuum thickness is larger than 1.8 nm (Fig. 3). Therefore, we add a vacuum layer of 2.0 nm onto the unit cell of the periodic slab in order to reduce the influence of the boundary condition on the computation procedure. A model for the UN(001) surface is plotted in Fig. 4.

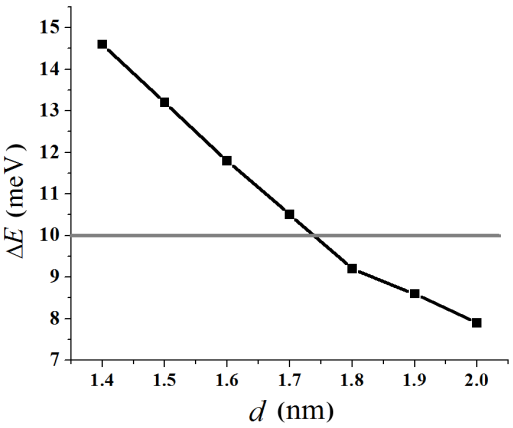

Fig. 3. Convergence test of the vacuum thickness for the UN(001) surface.

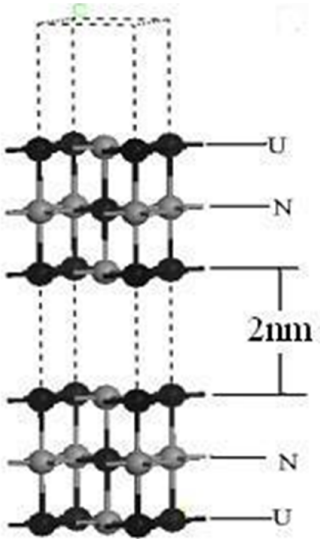

Fig. 4. A calculation model for the UN(001) surface.

The interactions of the surface atoms with UN matrix atoms will be unstable due to the absence of an adjacent atom, which is contrary to the matrix atoms. At the same time, these non-equilibrium interactions may cause the surface atoms to relax, reconstruct, find a new equilibrium site, and finally lower the total energy of the system. Moreover, this relaxation behavior may also change U-N bond length. A configuration model for relaxation calculation is shown in Fig. 2. In our work, relaxation is defined as relative change of U-N bond length, and the calculation result is listed in Table 1. From this table, we can see that the relative relaxation is relatively small (the maximum value at most 4.527%), so we fix the atoms in two low-lying layer in the following section, otherwise particularly declaration. For clarity, the configuration model and the relaxation calculation for the UN(111) surface are not shown here.

TABLE 1. Calculated results for configuration relaxation. R_i ($i = 1, 2$, in nm) and d_{ij} ($i = 1, 2$, $j = 1, 2$, in nm) represent U-N bond length in the intralayer and interlayer, respectively

$d_{\text{U-N}}$	After relaxation	Before relaxation	Relative relaxation (%)
R_1	0.244	0.243	0.041
R_2	0.242	0.243	−0.041
d_{11}	0.241	0.243	−0.082
d_{12}	0.237	0.243	−2.469
d_{21}	0.235	0.243	−3.292
d_{22}	0.232	0.243	−4.527

IV. RESULTS AND DISCUSSION

The energy minimum principle demonstrates that the higher the system symmetry, the lower the system energy, and the more stable the system. Therefore, we prefer an atom to be chemisorbed onto the high symmetrical position in the crystal surface. The UN crystal has fcc structure and several high symmetrical chemisorption positions exist on the crystal surface. As discussed above, we consider four representative positions in this work, namely Bridge, Hollow, U-top, and N-top. The chemisorbed atom is directly placed on the top of individual positions to study chemisorption behavior of the atom on these positions, as shown in Fig. 1. Chemisorption parameters not only include position, but also the orientation and height of the atom from the UN(001) and (111) surfaces, where chemisorption orientation is associated with the molecule structure and chemisorption height mainly depends on stability of the system.

A. H atom

We define chemisorption height h as the nearest distance for an H atom from UN(001) and UN(111) surfaces, and express it in terms of fractional coordinates. We optimize the H-UN(001)/UN(111) system with the minimum total energies (Table 2). The results for H chemisorption energies and Mulliken charges of individual configurations are listed in Table 3. As shown in Table 2, chemisorption heights of Bridge position are the same as Hollow position, and chemisorption energy differences are within several MeV. We think Bridge position to be equivalent with Hollow position. To

TABLE 2. Total energies of H-UN(001)/UN(111) systems with different chemisorption positions and heights. Numerical values for H-UN(111) system are listed in parentheses. Meanings for Bridge, Hollow, U-top and N-Top configurations are discussed in the text

Configuration	h (nm)	E_{system}(eV)
Bridge	0.263 (0.282)	−11569.569 (−3094.786)
	0.264 (0.283)	−11569.569 (−3094.776)
	0.265 (0.284)	−11569.576 (−3094.786)
	0.266 (0.285)	−11569.575 (−3094.775)
	0.267 (0.286)	−11569.571 (−3094.773)
Hollow	0.251 (0.282)	−11570.033 (−3094.776)
	0.252 (0.283)	−11570.037 (−3094.776)
	0.253 (0.284)	−11570.038 (−3094.786)
	0.254 (0.285)	−11570.037 (−3094.775)
	0.255 (0.286)	−11570.033 (−3094.773)
U-top	0.274 (0.324)	−11569.733 (−3093.689)
	0.275 (0.325)	−11569.742 (−3093.691)
	0.276 (0.326)	−11569.746 (−3093.691)
	0.277 (0.327)	−11569.744 (−3093.688)
	0.278 (0.328)	−11569.737 (−3093.687)
N-top	0.237	−11569.194
	0.238	−11569.229
	0.239	−11569.245
	0.240	−11569.244
	0.241	−11569.231

TABLE 3. Chemisorption configurations, chemisorption energies E_{C} (in kJ/mol) and Mulliken charges Q (in e) for H atom. Numerical values for H-UN(111) system are listed in parentheses. Meanings for Bridge, Hollow, U-top and N-Top configurations are discussed in the text

Configuration	E_{C} (kJ/mol)	$Q(e)$
Bridge	12.023 (11.532)	−0.229 (−0.341)
Hollow	13.058 (11.531)	−0.368 (−0.341)
U-top	11.893 (11.242)	−0.144 (−0.314)
N-top	10.602	0.206

verify this statement, we still consider Bridge, Hollow, and U-Top positions for C and O chemisorptions. The most stable position for H chemisorptions on the UN(001) and UN(111) surfaces are Hollow position (chemisorption energy 13.06 kJ/mol) and Bridge/Hollow position (chemisorption energy 11.532 kJ/mol), respectively.

To further understand interaction of H atoms with the UN(001) surface, we analyze the projected density of states (PDOS) before and after H chemisorption in terms of electronic structure calculations, as shown in Fig. 5(a)– 5(c). In fact, the ground state valence electronic configurations of U and N atoms are $5f^3 6d^1 7s^2$ and $2s^2 2p^3$, respectively. From the point of ionic bonding behavior, the U$6d$ and $7s$ electrons fill the N$2p$ states and the three U$5f$ electrons form the highest occupied molecular orbital (HOMO) [29]. The characteristic peak of H $1s$ PDOS in the energy range of 17.157 eV and 20.271 eV shifts towards lower energy band induced by H chemisorption (Fig. 5(a)) and expands its peak area, indicating that H atoms gain electrons as a result of chemisorption, which is in agreement with the Mulliken charge analysis (the third row in Table 3). We neglect other s, p orbitals in

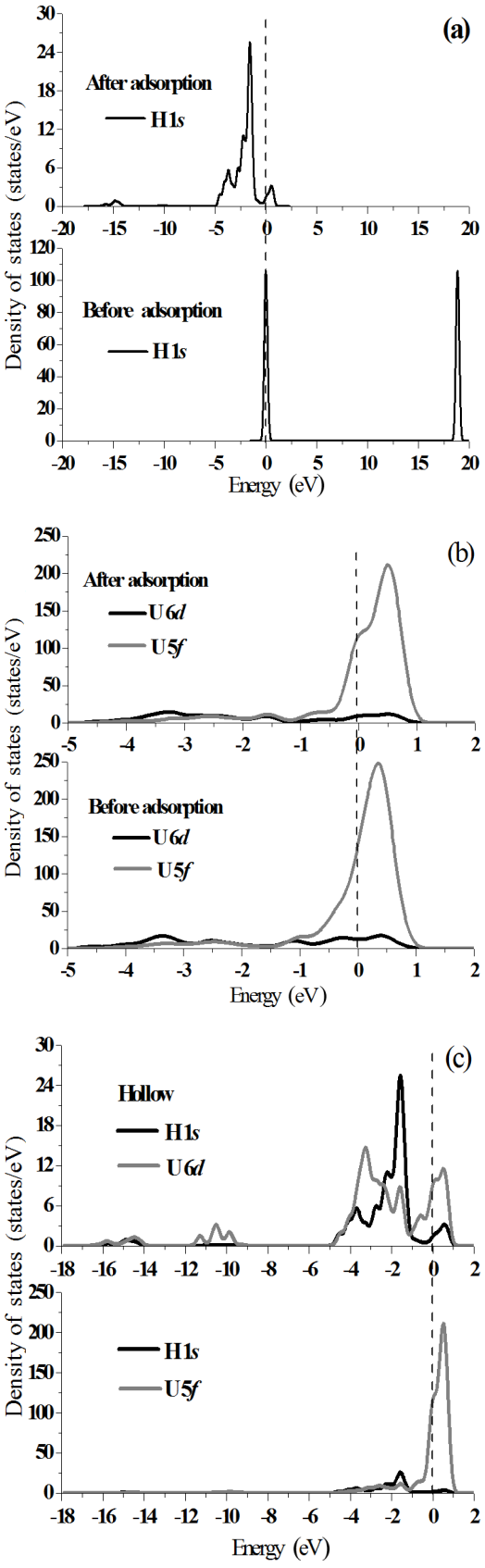

Fig. 5. Projected density of states (PDOS) of H $1s$ orbital (a), U $6d$, $5f$ orbitals (b) and H $1s$, U $6d$, $5f$ orbitals (c) before and after H chemisorption on the Hollow position of UN(001) surface. The Fermi energy (dash line) stands at 0 eV.

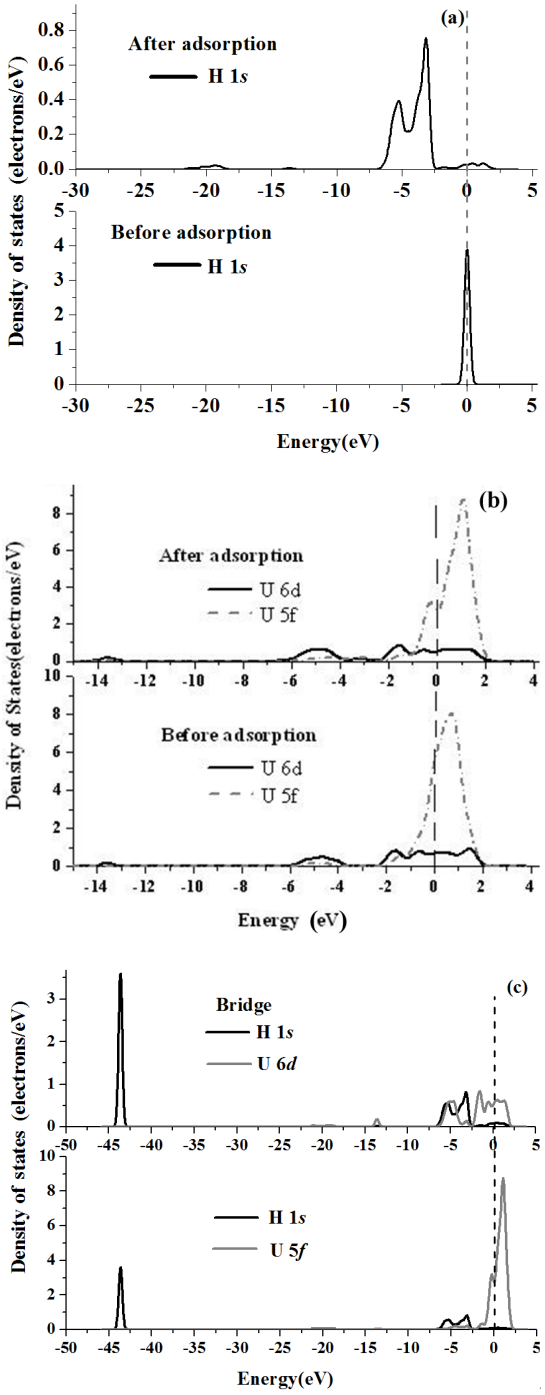

Fig. 6. Projected density of states (PDOS) of H $1s$ orbital (a), U $6d$, $5f$ orbitals (b) and H $1s$, U $6d$, $5f$ orbitals (c) before and after H chemisorption on the Bridge or Hollow positions of UN(111) surface. The Fermi energy (dash line) stands at 0 eV.

U atoms because $6d$, $5f$ orbitals dominate the structural and electronic properties of the U element.

We can see that H chemisorption causes the shape of U $5f$ PDOS with energy of -1.026 eV$\sim$0 eV to slightly change and peak position of U $5f$ PDOS shifts from 0.353 eV to 0.502 eV (Fig. 5(b)). From this plot we can see that peak

TABLE 4. Total energies of C-UN(001)/UN(111) systems with different chemisorption positions and heights. Numerical values for C-UN(111) system are listed in parentheses. Meanings for Bridge, Hollow, U-top and N-Top configurations are discussed in the text

Configuration	h (nm)	E_{system}(eV)
Bridge	0.253 (0.265)	-12587.704 (-3232.383)
	0.254 (0.266)	-12587.720 (-3232.386)
	0.255 (0.267)	-12587.727 (-3232.387)
	0.256 (0.268)	-12587.726 (-3232.384)
	0.257 (0.269)	-12587.719 (-3232.379)
Hollow	0.249 (0.265)	-12587.983 (-3232.383)
	0.250 (0.266)	-12587.995 (-3232.386)
	0.251 (0.267)	-12588.001 (-3232.387)
	0.252 (0.268)	-12588.000 (-3232.384)
	0.253 (0.269)	-12587.993 (-3232.379)
U-top	0.276 (0.314)	-12586.574 (-3229.448)
	0.277 (0.315)	-12586.578 (-3229.456)
	0.278 (0.317)	-12586.579 (-3229.459)
	0.279 (0.318)	-12586.574 (-3229.456)
	0.280 (0.319)	-12586.564 (-3229.447)
N-top	0.246	-12589.483
	0.247	-12589.528
	0.248	-12589.541
	0.249	-12589.527
	0.250	-12589.490

value decreases from 247.337 states/eV to 211.083 states/eV and peak area of U $6d$ PDOS obviously diminishes with energies of -1.042 eV and 1.515 eV, which show that U $6d$, $5f$ orbitals both lose electrons, also in agreement with the Mulliken charge analysis (Table 3). Fig. 5(c)) depicts H $1s$ and U $6d$, $5f$ PDOS. H $1s$ orbitals remarkably overlap with U $6d$ orbitals in the energy of -5.043 eV and 1.161 eV. However, H $1s$ orbitals almost separate from U $6f$ orbitals with energy intervals of -4.152 eV and -1.241 eV. It is known that the larger the overlapping area of PDOS, the higher the hybridized bonding. Therefore, the H atom will hybridize with the U atom as a consequence of H chemisorption. Electronic charges of U $6d$, $5f$ orbitals (mainly U $5f$ orbitals) transfer to the H $1s$ orbital, which is also consistent with the Mulliken charge analysis (Table 3).

Similarly, PDOSs before and after H chemisorption in Bridge or Hollow positions for the UN(111) surface are shown in Figs. 6(a)– 6(c). H chemisorption induces an H $1s$ peak around the Fermi level to the energy band in the energy range of -7.374 eV to -2.502 eV (Fig. 6(a)). However, H chemisorption has little effect on U $6d$, $5f$ PDOSs. U $6d$ states clearly hybridize with U $5f$ states between -2.215 eV and 2.00 eV, as shown in Fig. 6(b). H $1s$ states clearly overlap with U $6d$, $5f$ states (Fig. 6(c)), and acquire electrons from U atom, which is consistent with Mulliken analysis (Table 3).

B. C atom

Previous report [2] has shown that U carbides can effectively retard corrosion of U metal. The crystal structure of UN is the same as that of UC (NaCl type, face-

TABLE 5. Chemisorption configurations, chemisorption energies E_C (in kJ/mol) and Mulliken charges Q (in e) for C atom. Numerical values for C-UN(111) system are listed in parentheses. Meanings for Bridge, Hollow, U-top and N-Top configurations are discussed in the text

Configuration	E_C (kJ/mol)	$Q(e)$
Bridge	25.513 (24.132)	−0.400 (−0.543)
Hollow	18.81 (24.132)	−0.142 (−0.542)
U-top	15.69 (14.147)	−0.103 (−0.011)
N-top	25.502	−0.392

centered cubic structure) and the lattice constant is also very close to the latter (lattice constants of UN and UC are 0.4965 nm and 0.4889 nm, respectively). Therefore, we wonder whether chemisorption behavior of a C atom on UN(001) and UN(111) surfaces is also similar with that of a U monocarbide.

Next we perform electronic structure calculations of total energy for the C-UN(001)/UN(111) systems with different chemisorption positions and heights using the method discussed above and relax different configurations to find the optimal chemisorption positions and heights. The total energy results of the C-UN(001)/UN(111) systems are listed in Table 4. According to the chemisorption energy formula (Eq. (1)), a configuration with the maximum chemisorption energy is the most stable configuration for chemisorption on the UN(001) and UN(111) surface. Therefore, we optimize configurations with the minimum total energy for different chemisorption positions and the optimal configuration is the most stable configuration for certain chemisorption positions.

The chemisorption energy and Mulliken charge analysis results are presented in Table 5. From this table we can see that chemisorption energies reach the maximum value when the C atom chemisorbs or at the Bridge and N-top positions of the UN(001) surface (chemisorption energies are 25.513 kJ/mol and 25.502 kJ/mol, respectively). The chemisorption energy of the Bridge configuration is very close to that of the N-top configuration. The relaxtion calcultion shows that the former is unstable, and will transform to the latter. Therefore, the most stable configuration for C chemisorption on the UN(001) surface is N-top configuration. Similarly, relaxation result shows that the most stable configuration for C chemisorption on the UN(111) surface is the Bridge or Hollow configurations.

To further understand the interactions of C with the UN(001) and (111) surfaces, we analyze PDOS before and after C chemisorption in terms of electronic structure calculations, as shown in Figs. 7(a)– 7(d) and Figs. 8(a)– 8(d). C $2s$ and $2p$ PDOSs shift towards a lower energy band after chemisorption (Fig. 7(a)), and the peak area of C $2s$ and $2p$ PDOSs obviously increase, indicating that C atoms gain electrons from the adsorbate (UN(001) surface in the present work) as a result of chemisorption, which is in agreement with the Mulliken charge analysis (Table 5). U $6d$, $5f$ PDOSs before and after chemisorption are plotted in Fig. 7(b). C chemisorption has a negligible effect on U $6d$ PDOS, however, the peak value of the U $6d$ PDOS decreases (Fig. 7(b)), which shows that U $6d$ orbitals lose electrons. At the same time, C chemisorption also has a negligible effect on the U $5f$ PDOS in the energy interval of 0 eV∼1.520 eV. However, a new characteristic peak appears in the energy range of −1.0 eV∼0.50 eV, showing that U $5f$ orbitals hybridize with C $2s$ or $2p$ orbitals. As shown in Fig. 7(b), peak position of U $5f$ PDOS shifts from 0.508 eV to 0.572 eV and peak value decreases from 241.746 states/eV to 227.908 states/eV, indicating that U $5f$ orbitals also lose electrons. Figs. 7(c)– 7(d)) depict interactions of U $6d$, $5f$ orbitals with C $2s$, $2p$ orbitals. C $2s$ orbitals and U $6d$ orbitals produce a remarkable hybridization/mixing peak (Fig. 7(c)), while the C $2s$ PDOS almost separates from the U $5f$ PDOS. However, C $2p$ orbitals obviously overlap with U $6d$, $5f$ orbitals (Fig. 7(d)), showing that C $2p$ orbitals hybrid with U $6d$, $5f$ orbitals to form a covalent bond, which is in sharp contrast with Fig. 7(c). Therefore, electronic charges of U $6d$ orbitals transfer to C $2s$, $2p$ orbitals as a result of C chemisorption on the UN(001) surface and U $5f$ orbitals transfer to C $2p$ orbitals, these results are consistent with the Mulliken charge analysis (Table 5).

As shown in Fig. 8(a), C chemisorption widens the C $2p$ peak around the Fermi level, and new C $2s$ states appear in the energy interval of −5.241 eV∼−2.632 eV to −21.352 eV∼−18.471 eV (Fig. 8(a)). However, C chemisorption also has a negligible effect on U $6d$, $5f$ PDOSs (Fig. 8(b)). C $2s$ states slightly overlap with U $6d$, $5f$ states (Fig. 8(c)). However, C $2p$ states obviously hybridize with U $6d$, $5f$ states (Fig. 8(d)) and acquire a majority of electrons (about 2/3) from the U atom, which is consistent with Mulliken analysis (Table 5).

C. O atom

Previous report [30] has shown that H_2O chemisorption on U metal will result in the formation of UO_2 passivation film on the metal surface and that this film can prevent U metal from further oxidization. Therefore, investigation of O chemisorption on the UN surface may be helpful for understanding anti-corrosion mechanisms of U metal because UN passivation film is also a well-known corrosion-resistant material.

According to the minimum energy principle, the total energy of a system would be the minimum value for H_2O chemisorption on the optimal position and the system would be the most stable one. Therefore, we first perform total energy calculations for O-UN(001)/UN(111) systems with different chemisorption positions and heights, and then optimize several systems with the minimum energies (Table 6). The calculation results are listed in Table 7. From this table, we can see that the most stable configuration for O chemisorption on the UN(001) surface is Hollow configuration. O chemisorption induces the UN(001) surface to reconstruct, where U atoms move outwards and N atoms move towards the matrix, thereby causing U-N bond length to change. The maximum relative change for U-N bond length reaches 15.79%, indicating that O atom strongly interacts with the UN(001) surface (not shown here).

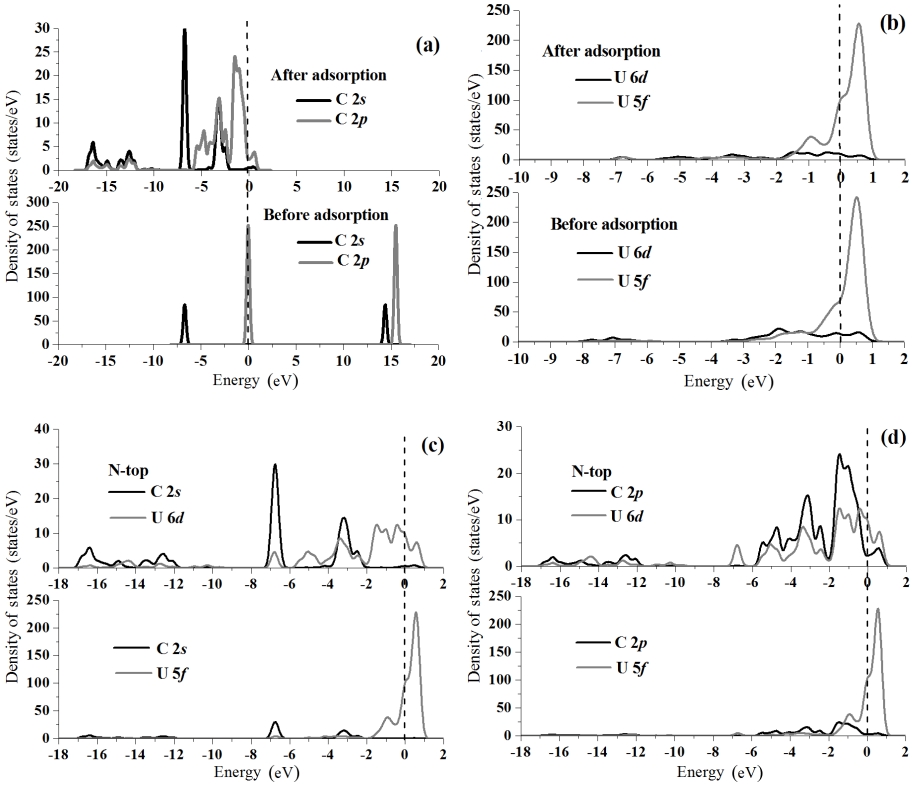

Fig. 7. Projected density of states (PDOS) of C $2s$, $2p$ orbital (a), U $6d$, $5f$ orbital (b), C $2s$, U $6d$, $5f$ orbital (c) and C $2p$, U $6d$, $5f$ orbital (d) before and after C chemisorption on N-top position of the UN(001) surface. The Fermi energy (dash line) stands at 0 eV.

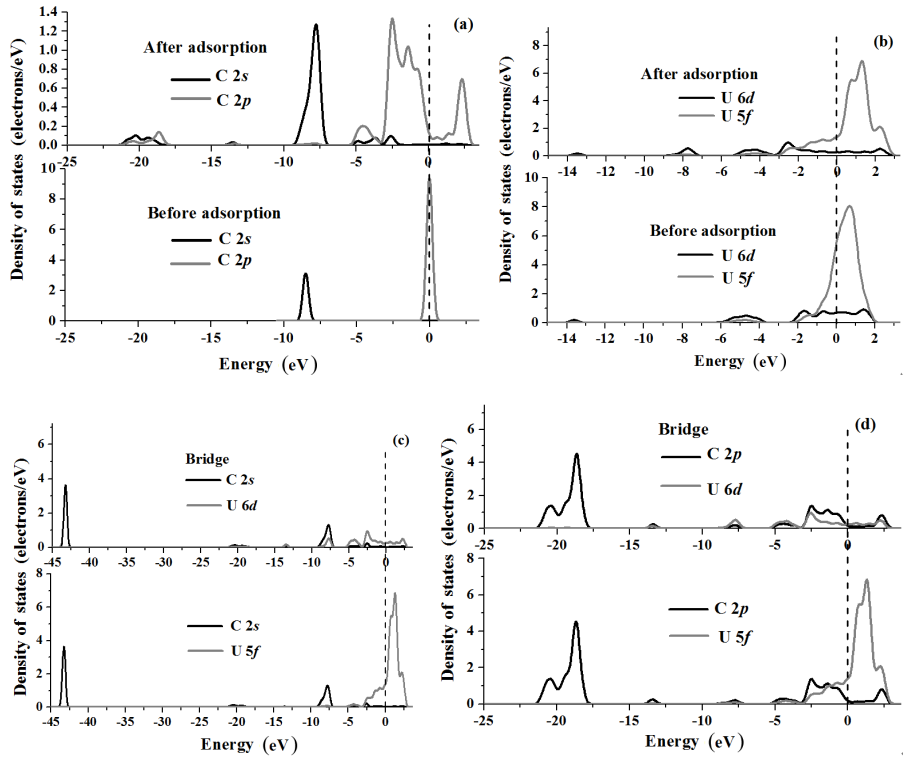

Fig. 8. Projected density of states (PDOS) of C $2s$, $2p$ orbital (a), U $6d$, $5f$ orbital (b), C $2s$, U $6d$, $5f$ orbital (c) and C $2p$, U $6d$, $5f$ orbital (d) before and after C chemisorption on Bridge or Hollow positions of the UN(111) surface. The Fermi energy (dash line) stands at 0 eV.

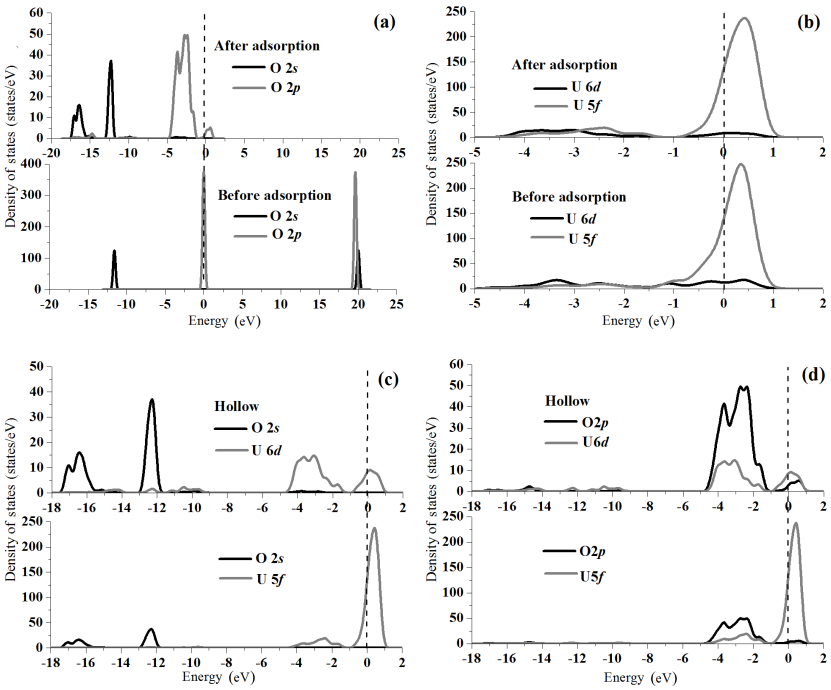

Fig. 9. Projected density of states (PDOS) of H $1s$, O $2s$, $2p$ orbital (a), U $6d$, $5f$ orbital (b), O $2s$, U $6d$, $5f$ orbital (c) and O $2p$, U $6d$, $5f$ orbital (d) before and after O_2 chemisorption on the BU position of the UN (001) surface. The Fermi energy (dash line) stands at 0 eV.

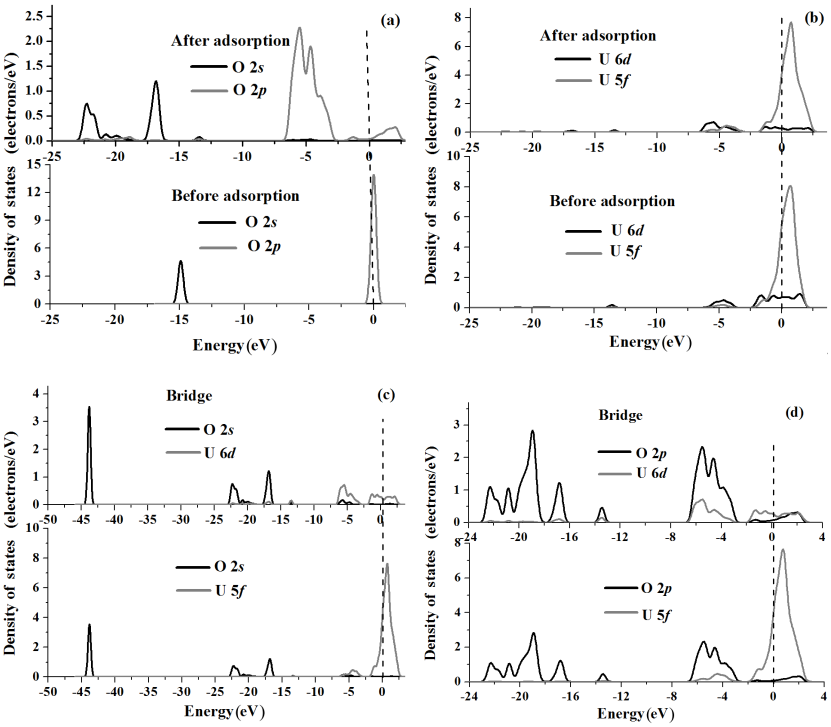

Fig. 10. Projected density of states (PDOS) of H $1s$, O $2s$, $2p$ orbital (a), U $6d$, $5f$ orbital (b), O $2s$, U $6d$, $5f$ orbital (c) and O $2p$, U $6d$, $5f$ orbital (d) before and after H_2O chemisorption on Bridge or Hollow positions of the UN(111) surface. The Fermi energy (dash line) stands at 0 eV.

TABLE 6. Chemisorption heights and chemisorption energies E_C (in kJ/mol) for O atom on UN(001) and UN(111) surafces. Numerical values for O-UN(111) system are listed in parentheses. Meanings for Bridge, Hollow, U-top and N-Top configurations are discussed in the text

Configuration	h (nm)	E_C (eV)
Bridge	0.256 (0.271)	−13601.973 (−3517.916)
	0.257 (0.272)	−13601.997 (−3517.921)
	0.258 (0.273)	−13602.008 (−3517.921)
	0.259 (0.274)	−13602.007 (−3517.918)
	0.260 (0.275)	−13601.994 (−3517.912)
Hollow	0.250 (0.271)	−13602.208 (−3517.916)
	0.251 (0.272)	−13602.284 (−3517.920)
	0.252 (0.273)	−13602.291 (−3517.921)
	0.253 (0.274)	−13602.290 (−3517.918)
	0.254 (0.275)	−13602.281 (−3517.912)
U-top	0.266 (0.310)	−13603.085 (−3516.680)
	0.267 (0.311)	−13603.141 (−3516.694)
	0.268 (0.312)	−13603.164 (−3516.696)
	0.269 (0.313)	−13603.160 (−3516.688)
	0.270 (0.314)	−13603.131 (−3516.647)
N-top	0.250	−13600.955
	0.251	−13600.984
	0.252	−13600.993
	0.253	−13600.984
	0.254	−13600.959

TABLE 7. Chemisorption energies E_C (in kJ/mol) and Mulliken charges Q (in e) for O atom

Configuration	E_C (kJ/mol)	$Q(e)$
Bridge	26.110 (28.973)	−0.275(−0.619)
Hollow	27.34 (28.972)	−0.573(−0.620)
U-top	26.263 (23.692)	−0.366(−0.284)
N-top	20.021	−0.406

V. CONCLUSION

We also performed electronic structure calculations for O chemisorption on the UN(001) and UN(111) surfaces, and depicted the PDOS before and after chemisorption in Figs. 9(a)–9(d) and Figs. 10(a)– 10(d). C $2s$ and $2p$ PDOSs shift towards a lower energy band after chemisorption (Fig. 9(a)) and the peak area of the C $2p$ PDOS increases, indicating that C atoms gain electrons from the UN(001) as a result of chemisorption, which is in agreement with the Mulliken charge analysis (the third row in Table 7). Peak areas of the U $6d$, $5f$ PDOS in the energy of -1.5 eV$\sim$1.3 eV diminish, which shows that U $6d$, $5f$ electrons transfer to the O $2s$ or $2p$ orbitals. However, peak areas of the U $6d$, $5f$ PDOS in the energy of -5.0 eV~-1.50 eV increase, indicating that U $6d$, $5f$ orbitals may hybridize with O $2s$ or $2p$ orbitals (Fig. 9(b)). The peak position of U $5f$ PDOS shifts from 0.354 eV to 0.418 eV, and the peak value decreases from 247.361 states/eV to 237.268 states/eV, implying that U $5f$ orbitals lose electrons. U $6d$ orbitals and O $2s$ orbitals form a relatively small overlapping peak, while the U $5f$ PDOS is almost separate from the O $2s$ PDOS (Fig. 9(c)). However, O $2p$ PDOS obviously overlap with U $6d$, $5f$ PDOSs (Fig. 9(d)), particularly the U $6d$ PDOS, which is in sharp contrast with Fig. 9(c). It is shown that the smaller the overlapping area, the weaker the chemical bonding and the lower the transferred charge. Therefore, electronic charges of U $6d$ orbitals transfer to O $2s$ and $2p$ orbitals (mainly O $2p$ orbitals) and U $5f$ orbitals transfer to O $2p$ orbitals, which is in agreement with the Mulliken charge analysis (Table 7).

From Fig. 10(a), we can see that O chemisorption shifts the O $2s$, $2p$ peak to a lower energy, and widens O $2p$ PDOS. However, O chemisorption has an ignorable effect on U $6d$, $5f$ PDOSs (Fig. 10(b)). O $2s$ states slightly overlap with U $6d$, $5f$ states (Fig. 10(c)). However, O $2p$ states remarkably hybridize with U $6d$, $5f$ states (Fig. 10(d)) and acquire electrons from the U atom, which is consistent with Mulliken analysis (Table 7).

In the present work, we performed density functional theory calculations for H, C, and O chemisorptions on UN(001) and UN(111) surfaces using the generalized gradient approximation (GGA) and revised Perdew-Burke-Ernzerhof (RPBE) exchange-correlation functional at a non-spin polarized level with a periodic slab model. The results show that Hollow, N-top, and Hollow chemisorption sites are the most stable sites for H, C, and O atoms chemisorbed on the UN(001) suraface, respectively. The calculated electronic density of states (DOS) demonstrate electronic charge transfer between s, p orbitals in chemisorbed atoms and U $6d$, $5f$ orbitals and transferred electronic charges agree with the Mulliken charge analysis. Electronic structure calculations of H, C and O atom chemisorption on Bridge, Hollow, and U-Top positions of the UN(111) surface indicate that Bridge position is equivalent with Hollow position, two symmetrical chemisorption positions exist on UN(111) surface, namely Bridge (or Hollow) and U-Top, and the most stable chemisorption position for H, C, and O atoms is Bridge (or Hollow) position.

In the future, we plan to investigate the chemisorption of other atoms or molecules on the surface of actinide compounds, especially promising nuclear fuels such as Pu and U compounds, providing corresponding anti-corrosion techniques, and improving operational life and efficiency for nuclear fuel.

ACKNOWLEDGMENTS

We would like to thank our colleagues for their helpful comments and suggestions on this manuscript.

[1] Kotomin E A and Mastrikov Yu A. J Nucl Mater, 2008, **377**: 492–495.

[2] Bocharov D, Gryaznov D, Zhukovskii Yu F, *et al*. Surf Sci, 2011, **605**: 396–400.

[3] Shuai M B, Hu H R, Wang X, *et al*. J Mol Struc-Theochem, 2011, **536**: 269–276.
[4] Dholabhai P P and Ray A K. J Alloy Compd, 2007, **444-445**: 356–362.
[5] Burns C J. Science, 2005, **309**: 1823–1824.
[6] Shibata H, Tsuru T, Hirata M, *et al*. J Nucl Mater, 2010, **401**: 113–117.
[7] Weck P F, Kim E, Balakrishnan N, *et al*. Chem Phys Lett, 2007, **443**: 82–86.
[8] Evarestov R A, Bandura A V, Losev M V, *et al*. J Comput Chem, 2008, **29**: 2079–2087.
[9] Petit L, Svane A, Szotek Z, *et al*. Phys Rev B, 2009, **80**: 045124.
[10] Sunder S and Miller N H. J Alloy Compd, 1998, **271**: 568–572.
[11] Brooks M S and Glotzel D. Physica B, 1980, **102**: 51–58.
[12] Brooks M S. J Phys F Met Phys, 1984, **14**: 639–640.
[13] Sedmidubsky D, Konings R J, Novak P. J Nucl Mater, 2005, **344**: 40–44.
[14] Kotomin E A, Grimes R W, Mastrikov Y, *et al*. J Phys-Condens Mat, 2007, **19**: 106208.
[15] Evarestov R A, Losev M V, Panin A I, *et al*. Phys Status Solidi B, 2008, **245**: 114–122.
[16] Czekata M S, Talik E, Troc R, *et al*. Phys Rev B, 2007, **76**: 144426.
[17] Fynn R A and Ray A K. Phys Rev B, 2007, **76**: 115101.
[18] Savrasov S Y and Kotliar G. Phys Rev Lett, 2000, **84**: 3670–3673.
[19] Reihl B, Hollinger G, Himpsel F J. Phys Rev B, 1983, **28**: 1490–1494.
[20] Ritchie A G. J Nucl Mater, 1981, **102**: 170–182.
[21] Winer K, Colmenares C A, Smith R L. Surf Sci, 1987, **183**: 67–99.
[22] Zhukovskii Yu F, Bocharov D, Kotomin E A, *et al*. Surf Sci, 2009, **603**: 50–53.
[23] Zhukovskii Yu F, Bocharov D, Kotomin E A. J Nucl Mater, 2009, **393**: 504–507.
[24] Tasker P W. J Phys C Solid State, 1979, **12**: 4977–4984.
[25] Wang Y and Sun Y. J Phys-Condens Mat, 2000, **12**: L311–L316.
[26] Hay P J and Martin R L. J Chem Phys, 1998, **109**: 3875–3881.
[27] Delley B. Phys Rev B, 2002, **66**: 155125.
[28] Huda M N and Ray A K. Physica B, 2004, **352**: 5–17.
[29] Marutzk M, Barkow U, Schoenes J, *et al*. J Magn Magn Mater, 2006, **299**: 225–230.
[30] Hodkin E N. J Nucl Mater, 1977, **67**: 171–180.